

Charge Compensation in Solid Solutions**

Moritz Schmidt, Thorsten Stumpf,* Maria Marques Fernandes, Clemens Walther, and Thomas Fanghänel

The formation of solid solutions is a very general concept in nature found in many geological mineral phases as well as in a variety of technical products from cement to semiconductors. As suggested by the term “solid solutions,”^[1] solutes (for instance trace metal ions) are incorporated in a solvent. However, in contrast to liquid solutions, the “solvent” is a solid (in the present case the mineral calcite). In recent years, solid solutions have gained increasing attention.^[2–4] However, some of the fundamental principles of their formation have not yet been understood.^[5–7] Among them is charge compensation: substitution of matrix ions by foreign ions of different charge (in the present case substitution of Ca^{2+} by Cm^{3+} or Eu^{3+} ions) requires compensation of the excess charge. Several competing mechanisms have been proposed,^[8–10] but to date none has been unambiguously proven or disproven. Herein, we demonstrate on a molecular level, exemplified by $\text{Cm}^{3+}/\text{Eu}^{3+}$ -doped calcite, that charge compensation is provided by the coupled substitution mechanism,^[10] that is, the simultaneous substitution of two Ca^{2+} by one Cm^{3+} and one Na^+ ion. Replacing Na^+ by the 30% larger K^+ during the synthesis of $\text{Eu}^{3+}/\text{Cm}^{3+}$ -doped calcites strongly decreases or even completely prevents the incorporation of the trivalent metal ions. The present results on the frequently discussed coupled substitution mechanism as a general charge-compensation mechanism help further understanding of the nature of substitutional solid solution formation by the great majority of natural and artificial mineral phases.

There is a wide range of solid solutions found both in the geosphere and in technical products. In nature, only very few minerals exist as a pure phase, while most represent solid

solutions of varying complexity (cf. the system calcite, dolomite, magnesian calcite in e.g. reference [11,12]). Furthermore, many technical products can be considered solid solutions; among them are (doped) semi- and superconductors,^[13–15] but also seemingly simpler cement.^[16,17]

Herein, we focus on calcite, one of the most widely distributed mineral phases in the earth's crust. Calcite is the thermodynamically stable modification of CaCO_3 and crystallizes in the trigonal space group $R\bar{3}c$. Each Ca^{2+} ion is surrounded by six carbonate groups, coordinating Ca^{2+} by one oxygen atom each, in an octahedral geometry. The point group of the Ca^{2+} lattice site is C_{3i} .^[18] Natural calcites contain a variety of impurities, among these many rare earth elements (REEs). It is well known that the distribution of impurities, and of the REEs in particular, allows us to draw conclusions on the environment and the conditions during formation and aging of calcite.^[10] To gain insight into the incorporation mechanisms and the charge compensation associated with it, we investigated synthetic calcites doped with Eu^{3+} or Cm^{3+} ions, which served as analogues for the natural solid solution calcite. Among the REEs, Eu^{3+} was chosen because of its convenient optical fluorescence. Time-resolved laser fluorescence spectroscopy (TRLFS) on Eu^{3+} is widely used as a versatile structural probe in crystalline and noncrystalline solids.^[19–24] The nondegeneracy of the Eu^{3+} ion's fluorescing states ($^5\text{D}_0 \rightarrow ^7\text{F}_0$) gives rise to a single emission line for each species and facilitates determination of the number of non-equivalent sites of the Eu^{3+} ion by simply counting the number of emission lines. Once the corresponding excitation energies (i.e. the peak maxima) have been derived from the excitation spectrum, each site can be excited selectively to record emission spectra of each site of a complex mixture separately, with high selectivity, and without interference from the others. In particular, the coordination symmetry of each site can be uniquely identified, since the splitting of the $^7\text{F}_2$ state is very sensitive to changes in the ligand field (so-called hypersensitivity).^[25] Likewise, the number of water molecules in the first coordination sphere of the metal ion is determined by selectively measuring the fluorescence intensity as a function of time after excitation. All measurements reported herein showed monoexponential functionality with decay rate k ,^[26] which correlates with the number of water ligands $n_{\text{H}_2\text{O}}$ in the first coordination sphere according to Horrocks' equation: $n_{\text{H}_2\text{O}} = 1.07k - 0.62$.^[27] However, the fluorescence of Eu^{3+} is rather weak and not suited to investigate doping at trace levels. By using its 5f homologue, the actinide curium, the detection limit of TRLFS is lowered to 10^7 atoms mm^{-2} , and even at Cm^{III} contents below 1 ppm, we are able to identify various Cm species spectroscopically.^[28–30] While there is no hypersensitive band in the case of

[*] M. Schmidt, Dr. T. Stumpf, Dr. C. Walther
Institut für Nukleare Entsorgung, Forschungszentrum Karlsruhe
Postfach 3640, 76021 Karlsruhe (Germany)
Fax: (+49) 7247-82-3927
E-mail: thorsten.stumpf@ine.fzk.de

Dr. M. Marques Fernandes
Laboratory for Waste Management, Paul Scherrer Institut
5232 Villigen (Switzerland)

Prof. Dr. T. Fanghänel
European Commission, Joint Research Centre
Institute for Transuranium Elements
Postfach 2340, 76125 Karlsruhe (Germany)

Dr. T. Stumpf, Prof. Dr. T. Fanghänel
Physikalisch-Chemisches Institut
Ruprecht-Karls-Universität Heidelberg
Im Neuenheimer Feld 253, 69120 Heidelberg (Germany)

[**] This work was cofinanced by the Helmholtz Gemeinschaft Deutscher Forschungszentren (HGF) by supporting the Helmholtz-Hochschul-Nachwuchsgruppe “Aufklärung geochemischer Reaktionsmechanismen an der Wasser/Mineralphasen Grenzfläche”.

Cm^{3+} , changes in the ligand field are detectable from spectral shifts of the (${}^6\text{D}_{7/2} \rightarrow {}^8\text{S}_{7/2}$) transition, and the number of water ligands can be determined in an analogous way to Eu^{3+} by use of Kimura's equation: $n_{\text{H}_2\text{O}} = 0.65k - 0.88$.^[31]

Calcite powders homogeneously doped with Eu^{3+} or $\text{Cm}^{3+}/\text{Gd}^{3+}$ were synthesized in a mixed-flow reactor under steady-state conditions (at constant pH value, ionic strength, and temperature). Each calcite is synthesized from three solutions: a Ca^{2+} solution, a $\text{Eu}(\text{ClO}_4)_3$ solution and a $\text{CO}_3^{2-}/\text{HCO}_3^-$ solution, which are pumped through the reactor in which the calcite seed is provided. The $\text{CO}_3^{2-}/\text{HCO}_3^-$ solution as well as the background electrolytes are prepared containing either Na^+ or K^+ in order to probe the possible influence of the electrolyte on charge compensation. Gd^{3+} was added to the Cm^{3+} -doped calcites to increase the number of trivalent cations to a total which exceeds the number of Na^+ contaminations from the K^+ reagents and the calcite seed crystals. Using only Cm^{3+} would lead to optical fluorescence quenching.

The ${}^7\text{F}_0 \rightarrow {}^5\text{D}_0$ excitation spectra of the Eu^{3+} -doped calcites exhibit three major peaks (Figure 1) corresponding to three non-equivalent sites A, B, and C. To probe the hydration state

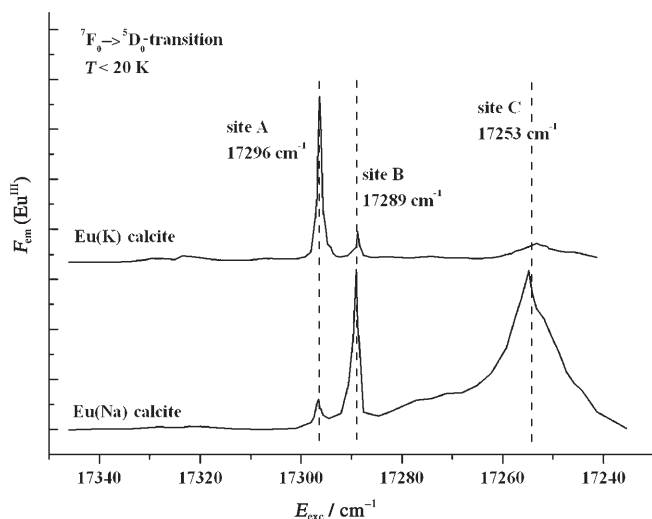


Figure 1. Excitation spectra of the ${}^7\text{F}_0 \rightarrow {}^5\text{D}_0$ transition in $\text{Eu}(\text{K})$ calcite and $\text{Eu}(\text{Na})$ calcite. Both spectra were recorded at temperatures below 20 K. $F_{\text{em}}(\text{Eu}^{\text{III}})$: normalized Eu^{III} fluorescence intensity; E_{exc} : excitation energy.

of each site, fluorescence lifetimes were recorded for selective excitation at 17296 (A), 17289 (B), and 17253 cm^{-1} (C). The relatively short lifetime $\tau_{\text{A}} = 400 \mu\text{s}$ ($k_{\text{A}} = 2500 \text{ s}^{-1}$) measured for site A indicates that one or two water molecules are coordinated to the metal ion (Horrocks' equation). In contrast, the fluorescence decay rates k_{B} and k_{C} are tenfold lower, indicating that no water is present in the first coordination shell of the metal ions at sites B and C (Table 1). This result suggests that in the case of A, a Eu^{3+} ion is sorbed to the calcite surface with remaining coordination by water, whereas sites B and C must be bulk lattice sites where the Eu^{3+} ions have lost their entire hydration sphere.

Table 1: Eu^{3+} and Cm^{3+} sites in calcite.

Site	Interaction	Symmetry	$k(\text{Cm calcite}), n(\text{H}_2\text{O})^{[a]}$	$k(\text{Eu calcite}), n(\text{H}_2\text{O})^{[a]}$
A	sorption	low	$1.220 \pm 165 \text{ s}^{-1}, 0.5$	$2.174 \pm 378 \text{ s}^{-1}, 1.5$
B	incorporation	low	$688 \pm 55 \text{ s}^{-1}, 0$	$277 \pm 34 \text{ s}^{-1}, 0$
C	incorporation	trigonal	$217 \pm 18 \text{ s}^{-1}, 0$	$273 \pm 16 \text{ s}^{-1}, 0$

[a] k : Decay constant of the $\text{Eu}^{3+}/\text{Cm}^{3+}$ fluorescence; the inverse of the fluorescence lifetime: $k = \tau^{-1}$.

Additional information is gained from the fine structure of the (${}^5\text{D}_0 \rightarrow {}^7\text{F}_2$) emission (Figure 2). The lower the symmetry of the Eu^{3+} site, the stronger the splitting of the observed bands; many symmetries can be identified unambiguously from typical splitting patterns.^[19–22,24–26] The emission spectra of both the surface site A and the first incorporation site B are strongly structured, showing the maximum possible splitting in all bands (F_1 : threefold, F_2 : fivefold), indicating low coordination symmetry (Figure 2a). In contrast, the emission

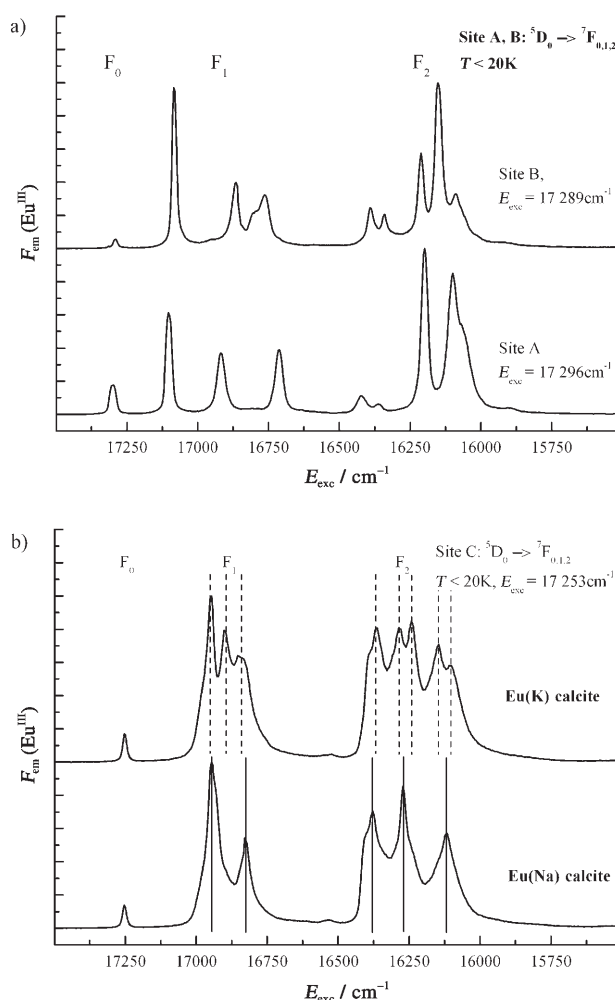


Figure 2. a) Fluorescence emission spectra of sites A and B in $\text{Eu}(\text{Na})$ calcite. Both spectra are strongly structured, showing maximum splitting in all bands. b) Fluorescence emission spectra of site C in both Eu calcite samples. The increased multiplicity of the signals for $\text{Eu}(\text{K})$ calcite is due to lowered symmetry caused by the lack of Na^+ .

pattern corresponding to site C shows only a twofold splitting of the ($^5D_0 \rightarrow ^7F_1$) and a threefold splitting of the ($^5D_0 \rightarrow ^7F_2$) band (Figure 2b), which is the typical pattern for C_{3i} symmetry only slightly deviating from the C_{3i} symmetry of the undisturbed Ca^{2+} lattice site in calcite.^[26] In short, we identified a surface site (site A) and two bulk incorporation sites; one of these is strongly distorted (site B), while the other is a nearly unaffected Ca^{2+} lattice site (site C).

In the case of Cm^{3+} -doped calcite, analogous sites are observed. As the spin-orbit coupling for 5f elements is stronger than for 4f elements, a stronger ligand field (increase in coordination strength) leads to a significant bathochromic shift ("red shift") of the ($^6D_{7/2} \rightarrow ^8S_{7/2}$) transition. In accordance with the stronger coordinative interaction of Cm^{3+} with CO_3^{2-} than with H_2O , the incorporation sites B and C (16213 cm^{-1} and 16015 cm^{-1} , respectively) are observed at lower energy than the surface site A (16526 cm^{-1} ; Figure 3). The assignment of the individual sites is corroborated by measurements of the lifetimes for each site, which are well in line with those measured for Eu^{3+} -doped calcites. All results concerning the species identification and characterization are summarized in Table 1.

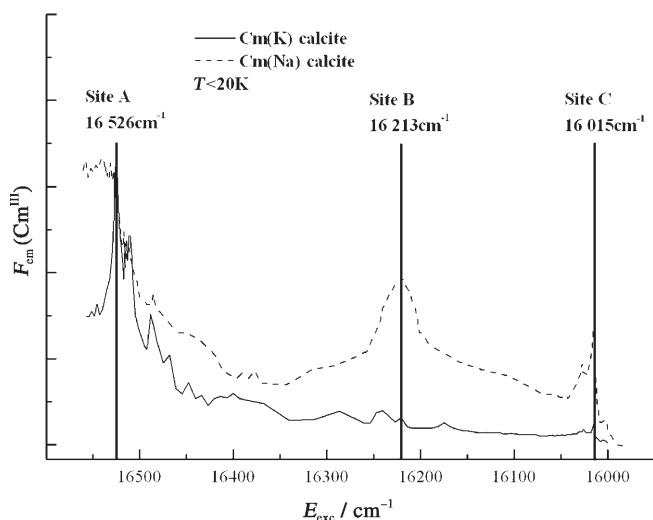


Figure 3. Excitation spectra of $Cm(K)$ calcite and $Cm(Na)$ calcite in the range $15980\text{--}16550\text{ cm}^{-1}$ at temperatures below 20 K .

Further experiments were performed to shed light on the charge compensation mechanism. If charge compensation was provided by formation of vacancies or incorporation of an anion (e.g. OH^-), a change of the electrolyte during sample preparation should have no effect. If, however, Na^+ was providing for charge compensation, substitution of Na^+ by the much larger K^+ ion should strongly affect charge compensation for both incorporation sites B and C. The K^+ ion is about one third larger than the almost equally sized ions Ca^{2+} , Na^+ , Eu^{3+} , Cm^{3+} , and Gd^{3+} (ionic radii in sixfold coordination (in pm):^[32] Ca^{2+} 114, Eu^{3+} 109, Cm^{3+} 111, Gd^{3+} 108, Na^+ 116, and K^+ 152) and hardly fits into a Ca^{2+} lattice site.

Comparing the excitation spectra of the samples synthesized with Na^+ ($Cm(Na)$ calcite) and K^+ ($Cm(K)$ calcite)

reveals the effect of this substitution most clearly (Figure 3). While in $Cm(Na)$ calcite a signal for each of the three sites A, B, and C is observed, the spectrum of $Cm(K)$ calcite shows only one prominent peak. The signal for the sorption site A is still present; however, none of the incorporation species' signals is detectable. Obviously, in the absence of Na^+ , compensation for the surplus charge of Cm^{3+} is no longer possible, thus strongly reducing incorporation in the calcite lattice bulk. Sorption onto the crystal's surface site A, as expected, is more flexible and thus not observably affected by the substitution of electrolyte.

Though incorporation of Eu^{3+} ions into sites B and C is strongly reduced as compared to the sample prepared in the presence of Na^+ , it is not completely suppressed, as revealed by the excitation spectrum of $Eu(K)$ calcite (Figure 1). Once again, we used the splitting of the ($^5D_0 \rightarrow ^7F_{0,1,2}$) emission bands after selective excitation of incorporation site C to gain information about the site's symmetry (Figure 2b). While the splitting pattern in the spectrum of $Eu(Na)$ calcite is typical for a C_{3i} symmetry (close to the Ca^{2+} lattice site's C_{3i} symmetry),^[26] the spectrum of $Eu(K)$ calcite shows the maximum splitting in both F_1 and F_2 transitions. This splitting is evidently caused by a reduction in the coordination symmetry of the Eu^{3+} ion arising from the replacement of Na^+ by K^+ . Either incorporation of the large K^+ ion or replacement of coupled substitution by an alternative mechanism for charge compensation (for example, formation of vacancies) will take place in direct proximity to a Eu^{3+} center and reduce the site's symmetry. The other incorporation species B does not show a comparable effect, which can be understood by considering the overall lower symmetry in this site.

Using site-selective time-resolved laser fluorescence spectroscopy, we observed a consistent set of effects caused by the substitution of Na^+ by K^+ in the growth solutions:

1. We observe a strong reduction of the amount of both incorporated Cm^{3+} species from $Cm(K)$ to $Cm(Na)$ calcite.
2. In the Eu calcites, we see a considerable change in the relative abundances of sorption and incorporation species: while the excitation spectrum of $Eu(K)$ calcite is dominated by the sorption species site A, the corresponding spectrum of $Eu(Na)$ calcite features the two incorporation sites B and C as most intense peaks with site A in a subordinate role.
3. The comparison of the emission spectra of site C in $Eu(Na)$ calcite and $Eu(K)$ calcite clearly shows an effect on the local symmetry of Eu^{3+} incorporated at this site. In the Na^+ system we observe a trigonal symmetry closely related to the C_{3i} symmetry of calcite's Ca^{2+} lattice site. This symmetry is disturbed in the K^+ system, as becomes obvious by the additional splitting in both F_1 and F_2 .

Since all these effects occurred after substituting the electrolyte Na^+ by K^+ while all other experimental parameters during calcite growth remained unchanged, obviously the presence of Na^+ is required for an effective incorporation of trivalent cations into calcite. Considering this dependence, it is reasonable to assume that Na^+ is providing for the required

charge compensation, that is, a Na^+ ion is incorporated in addition to each trivalent metal ion (Figure 4).

These results are of special significance, as they are not based on process-dependent macroscopic parameters but

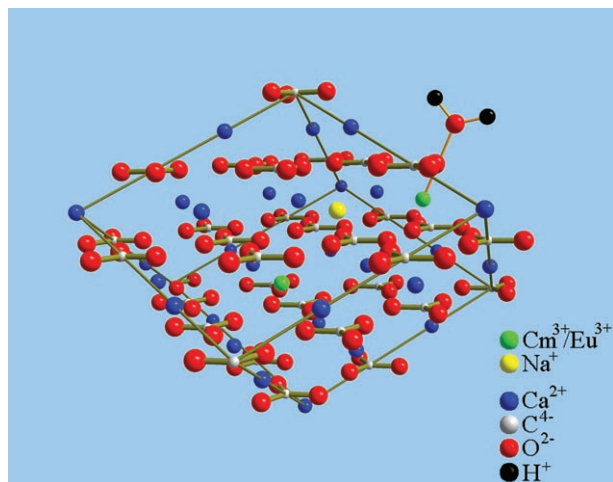


Figure 4. Schematic representation of the structure of the doped calcite. One trivalent cation (green, Cm^{3+} or Eu^{3+}) is incorporated into the bulk; its surplus charge is compensated by Na^+ (yellow) on a neighboring lattice site. Another trivalent cation is sorbed to the surface and coordinated by a water molecule.

were entirely derived from spectroscopic data. Moreover, calcite can be considered a model substance for simple crystalline systems. It represents a simple crystal lattice with only one well-defined cation site and no redox-active components. Systems of this kind do not offer a very widespread spectrum of options for charge compensation, and our results in the calcite system can surely be considered elementary. Still, as this mechanism has been discussed for several other systems besides calcite, such as powellite or apatite and more complex systems like $(\text{Na}_{1-x}\text{La}_x)(\text{Nb}_{1-(2x/3)}\text{Mg}_{2x/3})\text{O}_3$,^[33–35] these results will most likely find interest in a broad community and encourage further work in this field of research. These insights into the molecular processes of solid solution formation are expected to be useful in several fields, from basic mineralogy to semi- and superconductor studies and development of “intelligent barrier systems” for the geological long-term storage of nuclear waste.

Experimental Section

To achieve the desired spectral resolution, the calcite samples were cooled to temperatures below 20 K in a helium-refrigerated cryostat. The fluorescence was then excited by a XeCl excimer-pumped dye laser directly exciting the $\text{Eu}^{3+} {}^5\text{D}_0$ level or the $\text{Cm}^{3+} {}^6\text{D}_{7/2}$ level. The fluorescence emission signal was recorded in a time-resolved fashion by a fiber-coupled optical multichannel system consisting of a polychromator with 300, 600, and 1200 lines mm^{-1} gratings and diode array. In the case of the actinide, the isotope ^{248}Cm with a half-life of $T_{1/2} = 3.4 \times 10^5$ years was used.

For other applications of low-temperature TRLFS on Eu^{3+} and Cm^{3+} in crystalline host systems, see for example references [24,36].

Received: December 19, 2007

Revised: March 11, 2008

Published online: July 4, 2008

Keywords: actinoids · fluorescent probes · lanthanoids · laser fluorescence spectroscopy · solid solutions

- [1] A. J. Tesoriero, J. F. Pankow, *Geochim. Cosmochim. Acta* **1996**, 60, 1053.
- [2] J. Bruno, D. Bosbach, D. A. Kulik, A. Navrotsky, *Chemical Thermodynamics of Solid Solutions of Interest in Nuclear Waste Management*, Vol. 10, OECD Publishing, London, **2007**.
- [3] N. Mironova-Ulmane, V. Skvortsova, A. Kuzmin, U. Ulmanis, I. Sildos, E. Cazzanelli, G. Mariotto, *Phys. Solid State* **2005**, 47, 1516.
- [4] D. I. Woodward, J. Knudsen, I. M. Reaney, *Phys. Rev. B* **2005**, 72, 104110.
- [5] K. J. Davis, P. M. Dove, J. J. D. Yoreo, *Science* **2000**, 290, 1134.
- [6] A. G. Shtukenberg, Y. O. Punin, P. Azimov, *Am. J. Sci.* **2006**, 306, 553.
- [7] S. L. S. Stipp, J. Konnerup-Madsen, K. Franzreb, D. A. Kulik, H. J. Mathieu, *Nature* **1998**, 396, 356.
- [8] E. Curti, D. A. Kulik, J. Tits, *Geochim. Cosmochim. Acta* **2005**, 69, 1721.
- [9] L. Z. Lakshtanov, S. L. S. Stipp, *Geochim. Cosmochim. Acta* **2004**, 68, 819.
- [10] S. J. Zhong, A. Mucci, *Geochim. Cosmochim. Acta* **1995**, 59, 443.
- [11] R. S. Arvidson, F. T. Mackenzie, *Aquat. Geochem.* **2000**, 6, 249.
- [12] A. Mucci, *Aquat. Geochem.* **2004**, 10, 139.
- [13] C. L. Jia, M. Lentzen, K. Urban, *Science* **2003**, 299, 870.
- [14] S. Kang, A. Goyal, J. Li, A. A. Gapud, P. M. Martin, L. Heatherly, J. R. Thompson, D. K. Christen, F. A. List, M. Paranthaman, D. F. Lee, *Science* **2006**, 311, 1911.
- [15] D. H. Son, S. M. Hughes, Y. Yin, A. P. Alivisatos, *Science* **2004**, 306, 1009.
- [16] T. Matschei, B. Lothenbach, F. P. Glasser, *Cem. Concr. Res.* **2007**, 37, 118.
- [17] C. S. Walker, D. Savage, M. Tyrer, K. V. Ragnarsdottir, *Cem. Concr. Res.* **2007**, 37, 502.
- [18] R. Wartchow, *Z. Kristallogr.* **1989**, 186, 300.
- [19] K. Binnemans, C. Görller-Walrand, *J. Alloys Compd.* **1997**, 250, 326.
- [20] J. A. Capobianco, P. P. Proulx, N. Raspa, D. J. Simkin, D. Krashkevich, *J. Chem. Phys.* **1989**, 90, 2856.
- [21] H. Eilers, B. M. Tissue, *Chem. Phys. Lett.* **1996**, 251, 74.
- [22] V. Lavín, P. Babu, C. K. Jayasankar, I. R. Martin, V. D. Rodriguez, *J. Chem. Phys.* **2001**, 115, 10935.
- [23] V. Lavín, U. R. Rodriguez-Mendoza, I. R. Martin, V. D. Rodriguez, *J. Non-Cryst. Solids* **2003**, 319, 200.
- [24] B. Piriou, M. Fedoroff, J. Jeanjean, L. Bercis, *J. Colloid Interface Sci.* **1997**, 194, 440.
- [25] D. E. Henrie, R. L. Fellows, G. R. Choppin, *Coord. Chem. Rev.* **1976**, 18, 199.
- [26] C. Görller-Walrand, K. Binnemans in *Handbook on the Physics and Chemistry of Rare Earths* (Eds.: K. A. Gschneider, L. Eyring), Elsevier, Amsterdam, **1996**, p. 121.
- [27] W. D. Horrocks, Jr., D. R. Sudnick, *J. Am. Chem. Soc.* **1979**, 101, 334.
- [28] N. M. Edelstein, R. Klenze, T. Fanghänel, S. Hubert, *Coord. Chem. Rev.* **2006**, 250, 948.
- [29] P. Lindqvist-Reis, C. Apostolidis, J. Rebizant, A. Morgenstern, R. Klenze, O. Walter, T. Fanghänel, R. G. Haire, *Angew. Chem.* **2007**, 119, 937; *Angew. Chem. Int. Ed.* **2007**, 46, 919.

- [30] T. Stumpf, T. Fanghänel, *J. Colloid Interface Sci.* **2002**, 249, 119.
 - [31] T. Kimura, Y. Kato, H. Takeishi, G. R. Choppin, *J. Alloys Compd.* **1998**, 271–273, 719.
 - [32] R. D. Shannon, *Acta Crystallogr. Sect. A* **1976**, 32, 751.
 - [33] D. Bosbach, T. Rabung, F. Brandt, T. Fanghänel, *Radiochim. Acta* **2004**, 92, 639.
 - [34] M. Karbowiak, S. Hubert, *J. Alloys Compd.* **2000**, 302, 87.
 - [35] A. Sahu, O. M. Parkash, D. Kumar, *J. Mater. Sci. Lett.* **1997**, 16, 971.
 - [36] M. Illemassene, K. M. Murdoch, N. M. Edelstein, J. C. Krupa, *J. Lumin.* **1997**, 75, 77.
-